

Geophysical Research Letters[®]

RESEARCH LETTER

10.1029/2022GL099528

Special Section:

The First Results from the Emirates Mars Mission (EMM)

Key Points:

- We study a sequence of four Emirates Mars Mission images, showing a frontal dust cloud on 10 September 2021 (solar longitude 97)
- The dust cloud extends from the Chasma Boreale of the northern polar cap to the midlatitudes; it shows very little movement for 7–8 hr
- Large atmospheric fronts are unusual in this location and season; we discuss dynamical processes, supported by the Mars Climate Database

Supporting Information:

Supporting Information may be found in the online version of this article.

Correspondence to:

C. Gebhardt,
claus.gebhardt@uaeu.ac.ae

Citation:

Gebhardt, C., Guha, B. K., Young, R. M. B., & Wolff, M. J. (2022). A frontal dust storm in the northern hemisphere at solar longitude 97—An unusual observation by the Emirates Mars mission. *Geophysical Research Letters*, 49, e2022GL099528. <https://doi.org/10.1029/2022GL099528>

Received 10 MAY 2022

Accepted 5 OCT 2022

Author Contributions:

Conceptualization: C. Gebhardt

Data curation: M. J. Wolff

Formal analysis: B. K. Guha

Investigation: B. K. Guha

Methodology: C. Gebhardt

Visualization: C. Gebhardt





Writing – original draft: C. Gebhardt

Writing – review & editing: R. M. B. Young, M. J. Wolff

© 2022. The Authors.

This is an open access article under the terms of the [Creative Commons Attribution License](https://creativecommons.org/licenses/by/4.0/), which permits use, distribution and reproduction in any medium, provided the original work is properly cited.

A Frontal Dust Storm in the Northern Hemisphere at Solar Longitude 97—An Unusual Observation by the Emirates Mars Mission

C. Gebhardt^{1,2} , B. K. Guha² , R. M. B. Young^{1,2} , and M. J. Wolff³ 

¹Department of Physics, College of Science, United Arab Emirates University, Al Ain, United Arab Emirates, ²National Space Science and Technology Center, United Arab Emirates University, Al Ain, United Arab Emirates, ³Space Science Institute, Boulder, CO, USA

Abstract The Emirates Mars Mission (EMM) science phase began in Martian Year 36, solar longitude 49, which is outside of the classical Mars dust storm season. EMM observed a distinct dust cloud at northern mid-to-high latitudes on 10 September 2021 (Martian Year 36, solar longitude 97). The dust cloud is an arc-shaped dust storm, typically observed at the northern polar cap edge. This type of non-season dust storm is a well-known phenomenon, but this particular case is interesting because the dust cloud has frontal structure. A large atmospheric front is unusual in this location and season. Moreover, EMM's unique observational coverage adds value to this observation. EMM provided a sequence of four camera images, which are separated by just 2–3 hr. The dust cloud showed very little motion over 7–8 hr, that is, it is quasi-stationary. We discuss relevant dynamical processes, supported by a consistency check with the Mars Climate Database.

Plain Language Summary The Emirates Mars Mission (EMM) officially started its science observations on 23 May 2021. We saw some, but not many dust storms until end of 2021. That is because Mars has a dust storm season and a non-dust-storm-season, and EMM arrived during the latter. On 10 September 2021, EMM observed an arc-shaped dust storm close to the northern polar cap. This type of non-season dust storm is well-known. What makes this observation interesting is that the dust storm is also a weather front. A large atmospheric front is unusual for this location and time during the Martian year. Moreover, it is unique how EMM observed this dust storm. EMM took a camera image every 2–3 hr, giving four dust cloud images in total. The dust cloud showed very little motion over 7–8 hr. We discuss how the motion of air masses in the Mars atmosphere may have caused the observed dust storm. The discussion is supported by wind and temperature data from the Mars Climate Database.

1. Introduction

1.1. EMM Dust Storm Research

The United Arab Emirates operates the Emirates Mars Mission (EMM; Amiri et al., 2022; Almatroushi et al., 2021), which is the first Mars mission from an Arab country. The science phase of EMM officially began on 23 May 2021, which is equivalent to Martian Year 36, solar longitude 49 (MY36, $L_S = 49$).

The EMM science orbit varies between altitudes of around 20,000 km and 43,000 km. It has an orbital period of around 55 hr and a near-equatorial inclination of 25°. The orbit allows for snapshots of the Mars atmosphere and surface with a near-hemispheric view. Data products are obtained for a broad range of local solar times. As a result, EMM offers (sub-)diurnal, (sub-)seasonal, and annual data coverage.

The EMM camera EXI (Jones et al., 2021) is an imaging system with six spectral bands. There are three visible (VIS) bands centered near wavelengths of 635, 546, 437 nm and three ultraviolet (UV) bands centered near 320, 260, and 220 nm. These are also referred to as the f635, f546, f437, f320, f260, and f220 channels, respectively. The spatial image resolution varies between the periapsis and apoapsis of the EMM orbit, between around 2–4 km per pixel in the nadir looking direction. The ground size of a pixel increases by a factor of $1/\cos(\text{emission angle})$ for off-nadir looking direction.

The EXI primary science data are based on the XOS1 observation mode. An XOS1 data product is a sequence of VIS and UV images. The spatial binning is 2×2 pixels for f635 and UV images and 4×4 pixels for f546 and

f437 images. The aforementioned pixel ground size increases by a factor of 2 and 4, respectively. All EXI images considered in the following are XOS1 data products. We downloaded the level 2A images from the EMM Science Data Center (<https://sdc.emiratesmarsmission.ae/>).

1.2. Context Information on This EMM First Results Article

This article is part of the special collection “The First Results from the EMM.” The early part of the EMM science phase coincides with the low-dust-loading season (LDL) of MY36, from around $L_S = 10$ –140 (Montabone et al., 2020; Montabone & Forget, 2018). The LDL is known for the sparsity of dust storms at low-to-mid latitudes. Nonetheless, off-season dust storm activity around the Mars polar caps is common in the LDL. Polar cap edge dust storms are an annually recurring phenomenon (e.g., Battalio & Wang, 2021; Montabone et al., 2020).

EXI observed a distinct dust cloud on 10 September 2021 (MY36, $L_S = 97$) at northern mid-to-high latitudes. The dust cloud is an arc-shaped dust storm, typically observed at the northern polar cap edge. This type of dust storm is widely known, also in the northern hemisphere spring/summer from $L_S = 0$ –180 (Hinson & Wang, 2010; Guzewich et al., 2015; Sánchez-Lavega et al., 2018, 2022; Wang & Fisher, 2009; Wang & Richardson, 2015; among others). What makes this particular observation interesting is that the dust cloud has frontal structure. A large atmospheric front is unusual in this location and season. Moreover, EMM's unique observational coverage adds value to this observation. EMM provided a sequence of four images of this dust cloud, with a time separation of just 2–3 hr. The dust cloud shows very little motion over 7–8 hr, that is, it is quasi-stationary.

The structure of this article is as follows. Section 2 describes images from the EMM camera EXI and our dust storm identification method. Section 3 describes the studied dust storm and why its location and season are unusual. Section 4 discusses dynamical processes in the Mars atmosphere, which may have contributed to the observed dust storm. This is supported by a consistency check with the Mars Climate Database. A summary is given in Section 5.

2. Dust Storm Signatures in EMM Images

To identify dust storms from EMM/EXI images, we follow a methodology that is reminiscent of that in Cantor et al. (2001). Red-green-blue (RGB) composite images are examined for atmospheric features of any type. This includes both atmospheric dust features (i.e., dust storms and dust clouds) and water ice clouds. Each RGB image is constructed from a f635 (red), f546 (green), and f437 (blue) EXI image. The RGB images have a spatial binning of 4×4 pixels, which follows the native binning of the f546 and f437 images. We converted the spatial binning of f635 images from 2×2 to 4×4 pixels. To distinguish dust storms and water ice clouds, we compare f635 images with their f320 (UV) counterparts. Dust storms may be brighter than water ice clouds in f635 images (Cantor et al., 2001), because dust storms are usually optically much thicker than water ice clouds. Water ice clouds are similarly bright in the f635 and f320 images, whereas atmospheric dust is less bright in f320 images. That is because water ice clouds have a higher single scattering albedo than dust at UV wavelengths (Wolff et al., 2019).

As described above, the low-dust-loading season of MY36 was ongoing during the early EMM science phase. Until end of the year 2021, we identified several dust clouds, which extended from the Mars northern polar cap to lower latitudes. This is consistent with polar cap edge dust storms, which may dissipate toward the equator. One such dust cloud was particularly pronounced, and is the focus of this study. An advantage is that this dust cloud was observed from the most northerly position of the EMM orbit. As shown in Table 1, the sub-spacecraft latitude was close to the maximum possible of 25°N , which is determined by the orbital inclination of EMM. Geographic features of the northern polar cap, such as the Chasma Boreale, are under consideration in the following sections. An overview map including the northern polar cap is provided in Figure 1.

The identified frontal dust cloud was observed on 10 September 2021. It is visible in five RGB images from EXI, numbered here as Image1-5. Table 1 lists the associated f635 monochromatic images with their corresponding times in Earth UTC and Mars local true solar time at 50°W . Their f546, f437, and f320 counterparts are just seconds apart. Images1-4 show the dust cloud in high detail, around Mars local true solar times of 4,

Table 1
Five EXI Images Show a Frontal Dust Cloud on 10 September 2021

Image no.	Time of f635 image in Earth UTC (day, hour:minute:second)	Mars local true solar time at 50°W (decimal)	Sub-spacecraft latitude in °N	Sub-spacecraft longitude in °W	Spacecraft altitude in km
Image1	10 September 2021, 3:59:27	4.4	20.1	77.9	33,612
Image2	10 September 2021, 6:34:53	6.9	23.4	99.4	30,285
Image3	10 September 2021, 8:34:39	8.9	24.9	112.9	27,534
Image4	10 September 2021, 11:44:09	11.9	23.0	127.5	23,308
Image5	10 September 2021, 13:37:11	13.8	17.6	132.8	21,292

Note. These images are numbered as Image1–5. The image time is given in Earth UTC and Mars local true solar time at 50°W. Also, the sub-spacecraft latitude, sub-spacecraft longitude, and spacecraft altitude are provided.

7, 9 a.m., and 12 p.m. Even at the local true solar time of 4 a.m., most of the dust cloud is lighted by the Sun. Part of the dust cloud is in the polar day, given its solar longitude and northern latitudes. The polar day, that is, the absence of night at polar latitudes around summer solstice, is illustrated by the day-night-boundary in Figure 1.

A video animation of all five RGB images of the dust cloud is provided in Supporting Information S1. The dust cloud is still visible in the fifth image, but is very close to the limb, with commensurately lower detail. So, we include the fifth image in Supporting Information S1 and Table 1, but not in our analysis in the following sections. The dust cloud is an obvious atmospheric feature in the RGB images (Figure 2a), and remains distinct in the monochromatic f635 images (Figure 2b). While it is also visible in f320 images, it is clearly less pronounced (not shown). This supports our assertion that the frontal cloud is predominantly made of dust. Wang and Fisher (2009) reported that frontal events just before ~LS90-120 are predominantly dust storms. Frontal events after ~LS90-120 are predominantly ice clouds.

3. Expected and Unexpected Results From the Studied Dust Storm

As shown in Figure 3, the dust cloud extends from the polar cap edge southward, consistent with a northern summer polar cap edge dust storm. The long axis of the dust cloud is around 2,000 km, and the estimated area is around $5 \times 10^5 \text{ km}^2$. The dust cloud can hence be classified as a medium-to-large local dust storm. As expected, the dust cloud is smaller than a regional dust storm. By the definition of Cantor et al. (2001), regional dust storms have a minimum size of $1.6 \times 10^6 \text{ km}^2$. Regional dust storms are usual during northern hemisphere fall and winter.

The dust cloud has the typical structure of an atmospheric front. It is referred to as “frontal dust cloud” and “frontal dust storm” in this article. The fact that we observed a relatively large atmospheric front at $L_S = 97$ is unusual, within the context of the statistical occurrence of atmospheric fronts. This is detailed in the next two paragraphs.

First, the areal extent of $5 \times 10^5 \text{ km}^2$ is relatively large when compared with typical atmospheric fronts during northern hemisphere spring and summer. Figure 2 of Wang and Fisher (2009) records the sizes of 2,422 frontal events from $L_S = 0-180$ during Martian Years 24–28. Their areas vary between 740 km^2 and $1.5 \times 10^6 \text{ km}^2$, with a median of $6.9 \times 10^4 \text{ km}^2$. Only 89 frontal events, less than 10% of the total, have a size greater than $5 \times 10^5 \text{ km}^2$.

Second, it is known from climatological studies that northern polar atmospheric fronts are rare and, if present, small during $L_S = 90-120$. Based on Mars Daily Global Maps (MDGMs) of northern mid-to-high latitudes, Wang

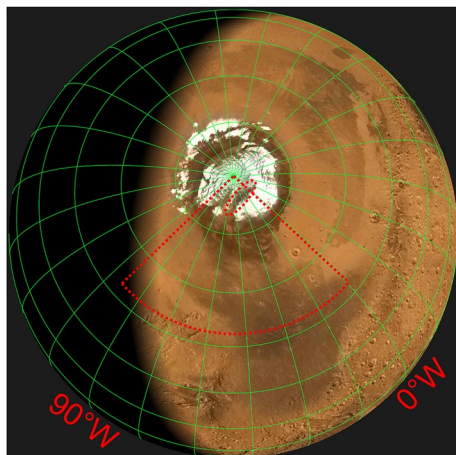


Figure 1. The Mars day and nightside are shown for 10 September 2021, 6:34:53 Earth UTC (the time of Image2 in Table 1). The surface topography is based on MOLA (Mars Orbiter Laser Altimeter; Smith et al., 2001). There is a latitude-longitude-grid with a spacing of 15°. The 0°W and 90°W lines are labeled. The Chasma Boreale of the northern polar cap is highlighted by an oval-shaped red line. The other red lines provide the approximate area of the map-projected EMM images in Figures 4a–4d. The latter show the frontal dust cloud under study. For orientation, an alternating pattern of bright and dark surface regions in the eastern part of Figures 4a–4d can be easily identified in the map above. The same is true for craters in the south-western part of Figures 4b–4d. Source: <https://www.giss.nasa.gov/tools/mars24/>.

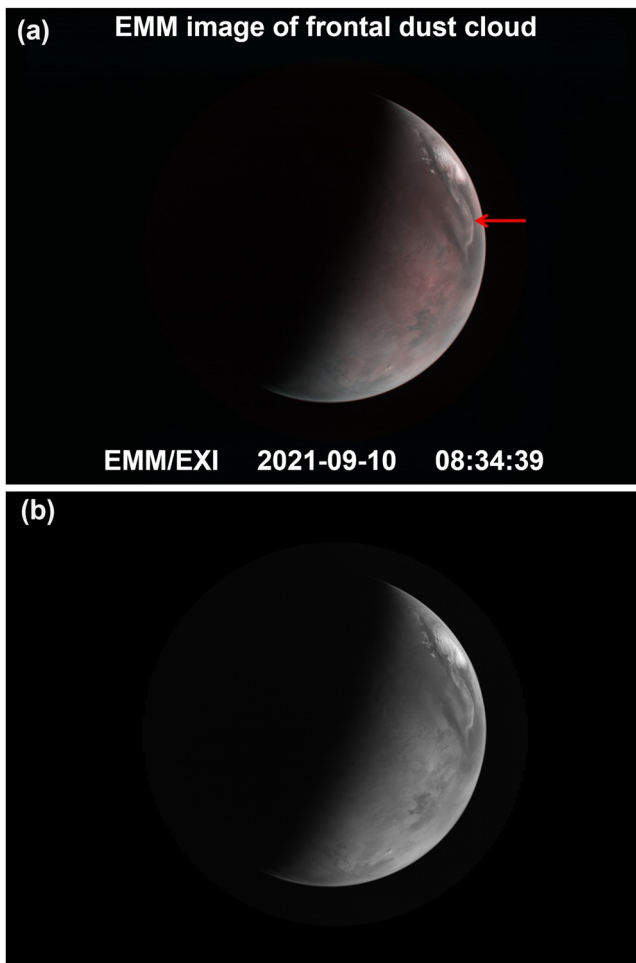


Figure 2. (a) RGB image from the EMM camera EXI from 10 September 2021, around 8:34:39 Earth UTC (MY36, $L_S = 97$). This is Image3, listed in Table 1. The image shows a distinct frontal dust cloud, highlighted by a red arrow. (b) Same as (a), but as a 635 nm monochromatic image.

and Fisher (2009) found that atmospheric fronts are rare and small during $L_S = 90$ –120. Some MDGMs are free of fronts and dust storms during this period. Large atmospheric fronts of $5 \times 10^5 \text{ km}^2$ and larger may occur shortly before, but typically not during $L_S = 90$ –120. Cantor et al. (2010) included MARCI/MRO observations. In relation to atmospheric fronts, they found that dust storm features are rare, and condensate cloud features may be absent around northern summer solstice (i.e., $L_S = 90$).

4. Discussion on Dust Storm Dynamics, Supported by the Mars Climate Database

The dust cloud does not show any signs of intensification or dissipation from Image1–4, as follows from Figure 3. Map-projected views of the frontal dust cloud are provided in Figure 4. The apparent lack of motion in these map projections indicates that the entire dust cloud is quasi-stationary for 7–8 hr. The dust cloud is predominantly oriented in the meridional direction. From the polar cap edge toward midlatitudes, the shape of the dust cloud is reminiscent of a question mark. At the northern end, the orientation of the cloud is south-eastward. With increasing distance from the polar cap, the direction of the dust cloud changes to south-westward. All directions here have a 180° ambiguity (the dust cloud could be also followed in south-to-north direction, which would give opposite directions).

A close look at Figures 2–4 reveals that the frontal dust cloud extends along the northern polar cap edge, from Chasma Boreale to the west. The width of the frontal dust cloud is several hundred kilometers. The latter follows from comparing it against the Chasma Boreale, whose main section is $\sim 60 \text{ km}$ wide (Fishbaugh & Head, 2002).

The dust cloud includes a coherent linear feature, oriented from the outlet of the Chasma Boreale south-westward. This is highlighted by a magenta line in Figures 4c and 4d. A close look suggests that the linear feature can be followed between Figures 4c and 4d. If correct, the motion of the linear feature is in an east-to-west direction. Tracking the feature yields a wind speed of $(5 \pm 1) \text{ m/s}$. The uncertainty of this estimate is a minimal error, given as image pixel size, divided by the time between the respective images. The motion in east-to-west direction by itself suggests the influence of near-surface winds. This follows from the fact that katabatic easterly winds at

around 80°N are confined to a narrow layer near the surface, as follows from Figure 4e. With increasing altitude, the easterly winds transition to the westerly direction, consistent with the thermal wind balance. Similar findings are reported in Tyler and Barnes (2014, 2005). Possibly, wind-driven surface dust lifting around the outlet of the Chasma Boreale contributes to the considered linear dust feature. This would be consistent with active aeolian scour, including erosion and transport of surface material, at northern polar scarps from the outlet of Chasma Boreale to the west (Warner & Farmer, 2008; their Figure 8).

Internal motion of the dust cloud throughout the image sequence needs to be estimated with care. Figures 4a–4d are dominated by changes in the boundary between day and night, solar illumination conditions, and the satellite viewing geometry. Moreover, the frontal dust cloud overlies certain bright features of the Mars surface in the images. In addition to the linear feature above, another distinct feature of the dust cloud is a bright blob near 60°W , 72°N . It can be followed between Figures 4b–4d, highlighted by a yellow circle. The blob moves toward the south-east between these three images, consistent with moving along the length direction of the dust cloud. Tracking the center of the blob from Figures 4b–4c and Figures 4c–4d yields wind speed estimates of $(7 \pm 2) \text{ m/s}$ and $(8 \pm 1) \text{ m/s}$, respectively. It is interesting that both estimates are consistent with one another. This adds credibility to the estimate and discussion in the paragraph before.

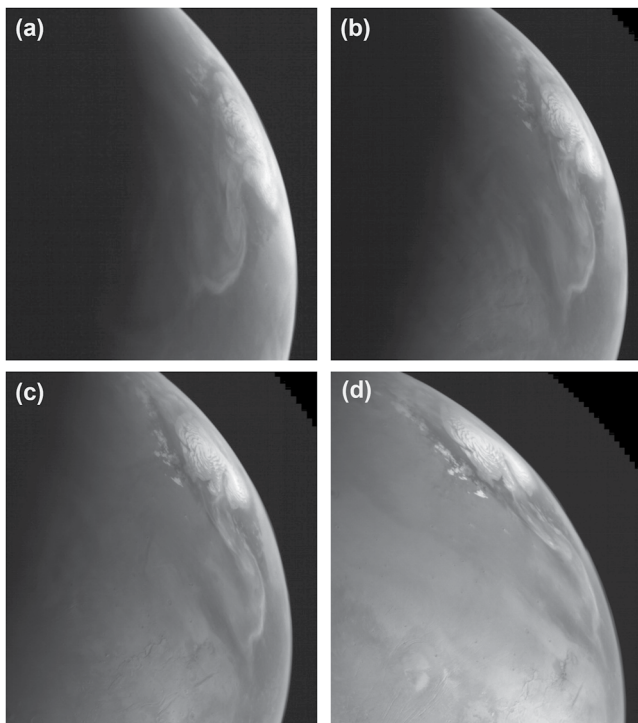


Figure 3. A magnified view of the frontal dust cloud under study, based on EXI monochromatic 635 nm images. Images (a–d), respectively, were obtained at 3:59, 6:35, 8:35, and 11:44 Earth UTC on 10 September 2021 (MY36, $L_S = 97$). These are Images 1–4, respectively, listed in Table 1.

As known from observations of the seasonal polar cap retreat (e.g., Appéré et al., 2011), the CO_2 ice has almost certainly fully retreated by the season studied here ($L_S = 97$). Hence, the polar ice cap that is present in the EMM images shown is the residual polar cap, made of water ice. By $L_S = 120^\circ$, the Coriolis effect may steer katabatic winds into anticyclonic circumpolar easterlies over the edge of the residual polar cap (Tyler & Barnes, 2005, 2014). A baroclinic zone around the residual polar cap and transient eddies at low altitude may develop because of the fairly sharp vertical wind shear and the asymmetric topography of the residual polar cap. The easterly winds near the surface transition into a weak westerly jet with increasing altitude, consistent with the thermal wind balance.

We performed a consistency check with the Mars Climate Database (MCD) for $L_S = 97^\circ$, using version 5.3 (as of Sep. 2022). Figure 4e shows the zonal wind (west-east wind component), based on the MCD climatology dust scenario with average solar activity, 50°W longitude, and diurnal averaging over all local times. The zonal wind has a discernible vertical gradient around 80°N . It transitions from easterly near the surface to westerly at higher altitudes. The latitude and strength of the vertical gradient have a certain degree of similarity with Tyler and Barnes (2014), their Figure 14a, right column, middle panel and Tyler and Barnes (2005), their Figure 8, first column from left, second panel. This suggests that baroclinic instability is non-negligible and could contribute to the frontal dust cloud under study.

Another factor could be the complex topography of Chasma Boreale. Shortly after $L_S = 90^\circ$, the northern polar atmosphere may have a wavenumber one synoptic structure (Tyler et al., 2008). This includes the possibility of stronger than normal winds blowing across the residual polar cap. Such winds may be enhanced, or diminished, by atmospheric flows associated with Chasma Boreale Tyler and Barnes (2005).

5. Summary

The EMM observed a distinct dust cloud on 10 September 2021 (MY36, $L_S = 97$). That was outside of the classical Martian dust storm season. The observed dust cloud is an arc-shaped dust storm, typically observed at the northern polar cap edge. This type of non-season dust storm is a well-known phenomenon, but this particular case is interesting because the dust cloud has frontal structure. A large atmospheric front is unusual in this location and season.

EMM's unique observational coverage adds value to this observation, by providing a sequence of four camera images of the frontal dust cloud, separated by 2–3 hr. The frontal dust cloud shows very little movement over 7–8 hr, that is, it is quasi-stationary. We estimated the wind speed and direction by tracking internal motion of the dust cloud. In one case, the estimated wind is consistent with near-surface easterly winds at the polar cap edge.

The article also discusses the connection between this dust storm and dynamical processes in the polar summer atmosphere. It is known a priori that the summer hemisphere only has a strong latitudinal temperature gradient close to the polar cap edge (Barnes et al., 2017). A consistency check with the Mars Climate Database supported that weak katabatic winds and baroclinicity are possible in the close vicinity of the polar cap edge. Also, the complex topography of Chasma Boreale of the northern polar cap is a possible factor.

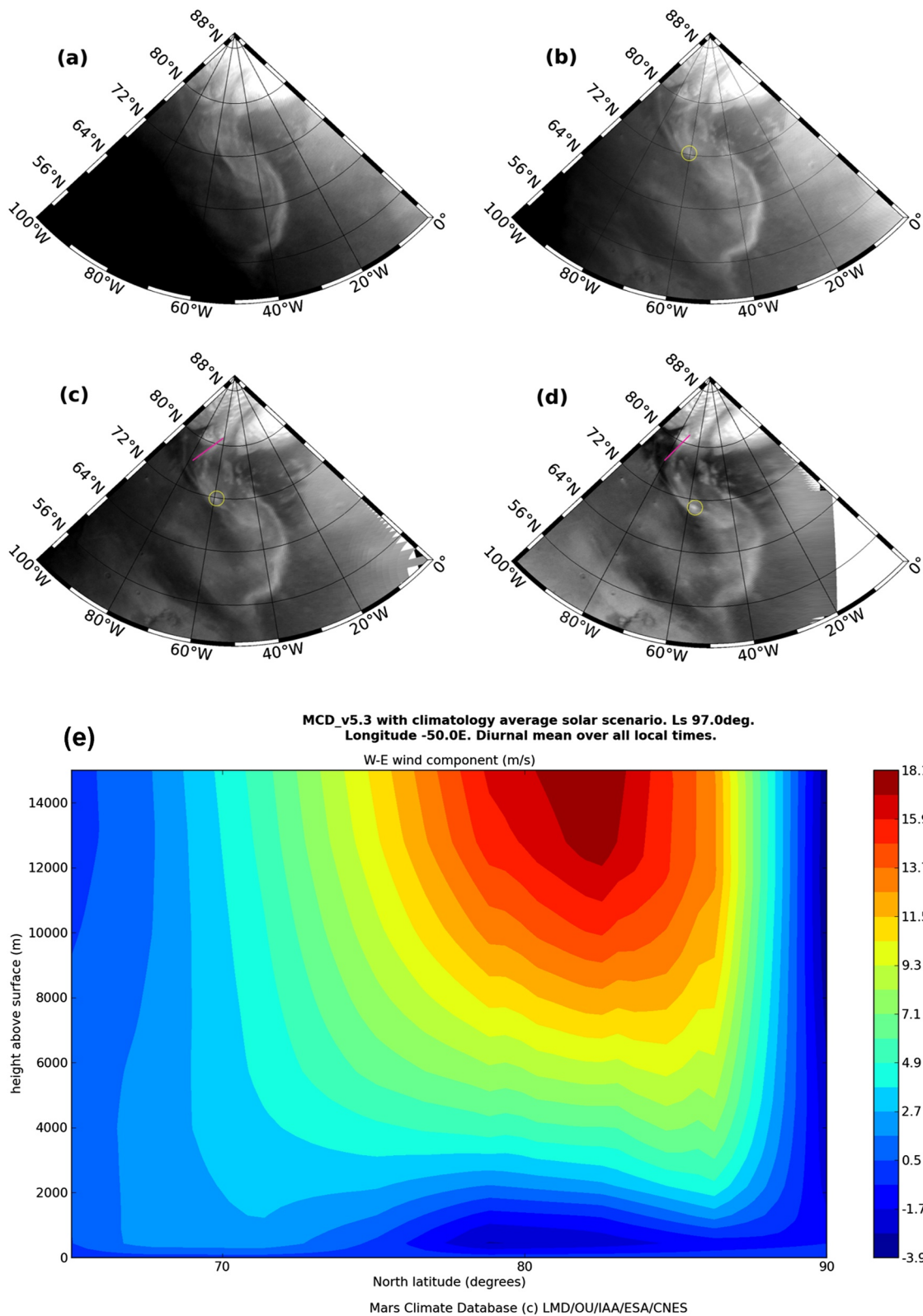


Figure 4. (a–d) are as Figure 3, but showing map-projected images. Each image includes a latitude-longitude-grid. The approximate area of (a–d) is highlighted by red lines in the map of Figure 1. Some dust storm features can be coherently tracked, such as a linear feature (magenta line) from (c–d) and a bright blob (yellow circle) from (b–d). (e) Shows the zonal wind (west-east wind component), based on the Mars Climate Database version 5.3, using the climatology dust scenario with average solar activity, $L_S = 97^\circ$, longitude $50^\circ W$, and diurnal averaging over all local times.

Data Availability Statement

The basis of this study are level2A images from the EMM camera EXI on 10 September 2021. All these images are publicly available from the EMM Science Data Center (<https://sdc.emiratesmarsmission.ae/>). The file names of the corresponding 635 nm monochromatic images include “emm_exi_l2a_20210910T035927_0105_xos1_f635,” “emm_exi_l2a_20210910T063453_0105_xos1_f635,” “emm_exi_l2a_20210910T083439_0105_xos1_f635,” “emm_exi_l2a_20210910T114409_0105_xos1_f635,” and “emm_exi_l2a_20210910T133711_0105_xos1_f635.” Their 546 nm, 437 nm, and 320 nm counterparts are just seconds apart. Data product filenames follow a standard convention: emm_<Instrument>_<DataLevel><StartTimeUTC>_<OrbitNumber>_<Mode>_<Description>_<KernelLevel>_<Version>.<FileType>.

Acknowledgments

Funding for the development of the EMM mission was provided by the United Arab Emirates Government, and to co-authors outside of the United Arab Emirates by the Mohammed Bin Rashid Space Centre. This work was also supported by a joint research agreement between the Mohammed Bin Rashid Space Centre and the National Space Science and Technology Center in the United Arab Emirates University, CG, BKG, and RMBY were supported by the United Arab Emirates University Grant “Mars and Earth atmospheric science research at the National Space Science and Technology Center,” G00003407. RMBY was also supported by UAE University grant G00003322.

References

- Almatroushi, H., AlMazmi, H., AlMheiri, N., AlShamsi, M., AlTunaji, E., Badri, K., et al. (2021). Emirates Mars mission characterization of Mars atmosphere dynamics and processes. *Space Science Reviews*, 217(8), 89. <https://doi.org/10.1007/s11214-021-00851-6>
- Amiri, H. E. S., Brain, D., Sharaf, O., Withnell, P., McGrath, M., Alloghani, M., et al. (2022). The emirates Mars mission. *Space Science Reviews*, 218(1), 4. <https://doi.org/10.1007/s11214-021-00868-x>
- Appéré, T., Schmitt, B., Langevin, Y., Douté, S., Pommerol, A., Forget, F., et al. (2011). Winter and spring evolution of northern seasonal deposits on Mars from OMEGA on Mars express. *Journal of Geophysical Research*, 116(E5), E05001. <https://doi.org/10.1029/2010JE003762>
- Barnes, J. R., Haberle, R. M., Wilson, R. J., Lewis, S. R., Murphy, J. R., & Read, P. L. (2017). The global circulation. In R. M. Haberle, R. T. Clancy, F. Forget, M. D. Smith, & R. W. Zurek (Eds.), *The atmosphere and climate of Mars*. Cambridge University Press. <https://doi.org/10.1017/9781139060172>
- Battalio, M., & Wang, H. (2021). The Mars dust activity database (MDAD): A comprehensive statistical study of dust storm sequences. *Icarus*, 354, 114059. <https://doi.org/10.1016/j.icarus.2020.114059>
- Cantor, B. A., James, P. B., & Calvin, W. M. (2010). MARCI and MOC observations of the atmosphere and surface cap in the north polar region of Mars. *Icarus*, 208(1), 61–81. <https://doi.org/10.1016/j.icarus.2010.01.032>
- Cantor, B. A., James, P. B., Caplinger, M., & Wolff, M. J. (2001). Martian dust storms: 1999 maorbiter camera observations. *Journal of Geophysical Research*, 106(E10), 23653–23687. <https://doi.org/10.1029/2000JE001310>
- Fishbaugh, K. A., & Head, J. W. (2002). Chasma boreale, Mars: Topographic characterization from Mars Orbiter Laser Altimeter data and implications for mechanisms of formation. *Journal of Geophysical Research*, 107(E3), 5013. <https://doi.org/10.1029/2000JE001351>
- Guzewich, S. D., Toigo, A. D., Kulowski, L., & Wang, H. (2015). Mars orbiter camera climatology of textured dust storms. *Icarus*, 258, 1–13. <https://doi.org/10.1016/j.icarus.2015.06.023>
- Hinson, D. P., & Wang, H. (2010). Further observations of regional dust storms and baroclinic eddies in the northern hemisphere of Mars. *Icarus*, 206(1), 290–305. <https://doi.org/10.1016/j.icarus.2009.08.019>
- Jones, A. R., Wolff, M., Alshamsi, M., Osterloo, M., Bay, P., Brennan, N., et al. (2021). The emirates exploration imager (EXI) instrument on the emirates Mars mission (EMM) hope mission. *Space Science Reviews*, 217(8), 81. <https://doi.org/10.1007/s11214-021-00852-5>
- Montabone, L., & Forget, F. (2018). Forecasting dust storms on Mars: A short review. In G. S. Levine, D. Winterhalter, & R. L. Kerschmann (Eds.), *Dust in the atmosphere of mars and its impact on human exploration*. Cambridge Scholars Publishing.
- Montabone, L., Spiga, A., Kass, D. M., Kleinboehl, A., Forget, F., & Millour, E. (2020). Martian year 34 column dust climatology from Mars climate sounder observations: Reconstructed maps and model simulations. *Journal of Geophysical Research: Planets*, 125(8), e2019JE006111. <https://doi.org/10.1029/2019JE006111>
- Sánchez-Lavega, A., Chen-Chen, H., Ordoñez-Etxeberria, I., Hueso, R., del Río-Gaztelurrutia, T., Garro, A., et al. (2018). Limb clouds and dust on Mars from images obtained by the visual monitoring camera (VMC) onboard Mars Express. *Icarus*, 299, 194–205. <https://doi.org/10.1016/j.icarus.2017.07.026>
- Sánchez-Lavega, A., Erkoreka, A., Hernández-Bernal, J., del Río-Gaztelurrutia, T., García-Morales, J., Ordoñez-Etxeberria, I., et al. (2022). Cellular patterns and dry convection in textured dust storms at the edge of Mars North Polar Cap. *Icarus*, 387, 115183. <https://doi.org/10.1016/j.icarus.2022.115183>
- Smith, D. E., Zuber, M. T., Frey, H. V., Garvin, J. B., Head, J. W., Muhleman, D. O., et al. (2001). Mars orbiter laser altimeter: Experiment summary after the first year of global mapping of Mars. *Journal of Geophysical Research*, 106(E10), 23689–23722. <https://doi.org/10.1029/2000JE001364>
- Tyler, D., & Barnes, J. R. (2005). A mesoscale model study of summertime atmospheric circulations in the north polar region of Mars. *Journal of Geophysical Research*, 110(E6), E06007. <https://doi.org/10.1029/2004JE002356>
- Tyler, D., & Barnes, J. R. (2014). Atmospheric mesoscale modeling of water and clouds during northern summer on Mars. *Icarus*, 237, 388–414. <https://doi.org/10.1016/j.icarus.2014.04.020>
- Tyler, D., Barnes, J. R., & Skillingstad, E. D. (2008). Mesoscale and large-eddy simulation model studies of the Martian atmosphere in support of Phoenix. *Journal of Geophysical Research*, 113(E8), E00A12. <https://doi.org/10.1029/2007JE003012>
- Wang, H., & Fisher, J. A. (2009). North polar frontal clouds and dust storms on Mars during spring and summer. *Icarus*, 204(1), 103–113. <https://doi.org/10.1016/j.icarus.2009.05.028>
- Wang, H., & Richardson, M. I. (2015). The origin, evolution, and trajectory of large dust storms on Mars during Mars years 24–30 (1999–2011). *Icarus*, 251, 112–127. <https://doi.org/10.1016/j.icarus.2013.10.033>
- Warner, N. H., & Farmer, J. D. (2008). Importance of aeolian processes in the origin of the north polar chasmata, Mars. *Icarus*, 196(2), 368–384. <https://doi.org/10.1016/j.icarus.2007.08.043>
- Wolff, M. J., Clancy, R. T., Kahre, M. A., Haberle, R. M., Forget, F., Cantor, B. A., & Malin, M. C. (2019). Mapping water ice clouds on Mars with MRO/MARCI. *Icarus*, 332, 24–49. <https://doi.org/10.1016/j.icarus.2019.05.041>